Centrifuge study of tunnel movements and their interaction with structures

P. Caporaletti & A. Burghignoli
University of Rome "La Sapienza", Rome, Italy

R.N. Taylor
City University, London, UK

ABSTRACT: The prediction of surface and subsurface ground displacements and strains is an important element in the design of new underground construction in urban areas. A number of plane strain centrifuge tests were undertaken at the City University, London, to model the effect of a tunnel excavation in layered ground consisting of a moderately stiff clay stratum overlain by a thick stratum of medium dense sand and the interaction of tunnelling generated ground movements on pre-existing structures. Tunnelling was performed beneath a buried thin and high structure founded close to the tunnel crown. The purpose of the study was to assess ground movements and strains at different depths and the potential damage on the pre-existing structure.

1 INTRODUCTION

The increasing demands of infrastructure development often require new excavations and especially tunnelling in urban areas for underground lines. The phenomena of ground-structure interaction due to tunnel excavation, including both ground displacements and strains and the assessment of damage on pre-existing structures are significant issues that need to be considered. The problem becomes particularly relevant when it involves layered ground and historical and archaeological structures, especially if they are buried within the soil. It is difficult to define their complex geometry and to investigate on their usually poor mechanical behaviour. Hence centrifuge testing, described in this paper, has been used to study the problem of tunnelling in layered ground and its effects on pre-existing structures, by modelling a completely buried thin "historical wall" perpendicular to the tunnel axis. The research work was intended to model real aspects of the new Metro C line in Rome.

The study of ground movements due to tunnel excavation is clearly a three-dimensional problem. But, with the exception of the volume loss at the tunnel face, the general analysis considers only the plane perpendicular to the tunnel axis and ground displacements and strains can thus be studied in a plane condition as for the greenfield configuration. However, pre-existing structures placed on or within the ground make the configuration more complex. In this study only the phase of tunnel excavation per-formed under a short time condition is considered, neglecting the effects of any consolidation process.

2 CENTRIFUGE MODELLING

2.1 *Principles of centrifuge modelling*

Centrifuge modelling represents a useful tool for investigating geotechnical problems. In contrast to conventional laboratory testing, it allows complex problems involving large ground volumes to be studied. Centrifuge modelling aims to maintain equality of effective stress and strains distributions in the model and equivalent prototype. The main principle is therefore the vertical stress σ_p at the prototype depth, h_p, should equal to the vertical stress σ_m at the corresponding model depth, h_m: $\sigma_p = h_p g = \sigma_m = h_m Ng$. thus with a model acceleration of Ng, $h_p = h_m N$. This definition of the scale factor, N, leads to other scaling laws for all parameters of interest: lengths are reduced N times from prototype to model, forces N^2, etc. (Taylor 1995).

2.2 *Centrifuge model*

The centrifuge tests were performed at the Geotechnical Research Centre, City University, London, on the Acutronic 661 Geotechnical Centrifuge, which is an asymmetric beam centrifuge with a swinging platform.

Equipment geometries and procedures were chosen to minimize scaling effects when considering lateral

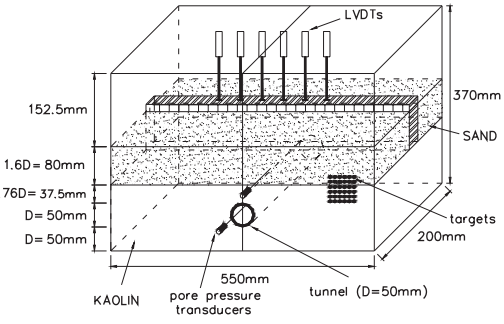

Figure 1. Schematic of centrifuge model.

acceleration, Coriolis acceleration, influence of grain size and boundary conditions. The tunnel was located in the middle of a kaolin stratum and the wall was placed far enough from both front and rear sides of container.

Figure 1 shows a schematic of the centrifuge model used to investigate the problem of tunnelling induced movements in a layered ground: the stratum of medium dense sand (Dr = 60–70%) overlies the layer of clay (OCR = 1.4–2.8). The wall made specifically for this research work, models a real structure buried almost completely within the sandy layer. A number of tests were carried out at the same scale factor N = 160. The first modelled the greenfield condition and subsequent tests used model walls of different strength and stiffness to investigate the wall interaction problem. The kaolin clay was initially consolidated to a vertical stress of 500 kPa inside the rectangular – $550 \times 200 \times 370\,mm^3$ – shown in Figure 1. The final clay depth of about 137.5 mm represented a 22 m layer at the prototype scale. The tunnel of circular shape – D = 50 mm – was cut in the kaolin layer and lined with a rubber bag and represented a real tunnel of diameter equal to 8 m and axis at about 23 m from the ground surface. The model wall, placed perpendicular to the tunnel axis was a right-angled parallelepiped $550 \times 25 \times 95$ and extended 15 mm out of the ground. It corresponded to a prototype wall 15.2 m high and 4 m width. It was placed within the upper sand layer that was 80 mm deep, i.e. 12.8 m prototype scale – with its foundation just at the sand/clay interface.

The air pressure in the tunnel liner bag controlled to equal the vertical total stress at tunnel axis level as the centrifuge speed was increased to give N = 160. Reducing the air pressure simulated the excavation process LVDTs measured vertical displacements on the ground surface, at the sand/clay interface and on the top of the model wall. Pore pressure transducers measured the excess pore pressure in the clayey stratum and in the external standpipe used to fix the hydraulic condition of the model. Black targets pressed into the frontal face of the model on a regular 10 mm grid were clearly visible in stored images. Subsequent digital image analysis allowed widespread fields of ground movements all around the tunnel to be determined.

2.3 *Materials used*

The upper stratum of cohesionless material was modelled by using Oakamoor HPs sand, a medium, uniform silica sand chosen for its light colour suitable to obtain a good contrast between targets and soil during images processing. Standard laboratory tests and direct shear tests gave the characteristic value of grain size $D_{50} = 0.238$, specific gravity $G_s = 2.654$, minimum void ratio $e_{min} = 0.6341$, maximum void ratio $e_{max} = 0.8828$, effective friction angle $\varphi' = 36°$ (loose sand) and $\varphi'_p = 42°$ and $\varphi'_{cv} = 36°$ (dense sand). Further drained triaxial tests and resonant column tests were also undertaken to have information about its stress-strain behaviour and on the shear stiffness at very small deformations.

Speswhite kaolin was used to model the clay soil. Its relative high permeability allows rapid dissipation of excess pore pressures during consolidation on the centrifuge. The main characteristics of the clay can be found in (Grant 1998).

Four model-walls were made for this research using mixtures of ordinary Portland cement EN 197-1 CEM1 42.5 N, hydrated lime BS 890, silica sub-rounded sand – both fine Leighton Buzzard sand and medium Oakamoor HPs sand – and distilled water. Different mixes produced model walls of different structures in terms of stiffness and strength, defined at an age of 5–6 days. The ratios of materials used were: lime/cement = 0.8 − 3, sand/cement = 1.1–6, water/cement = 1.5–5 and water/aggregates = 0.83 − 1.25. A number of laboratory tests were also carried out on cubes of size 100 mm and 23 mm in order to define the mechanical behaviour of the model-walls, which were in the ranges: compressive strength $\sigma_m = 0.5$–3.2 MPa, Young's modulus of initial stiffness $E_m = 18$–121 MPa, and unit weight $\gamma_m = 11.5$–$13.0\,kN/m^3$.

2.4 *Procedures*

The kaolin powder was mixed with distilled water (w = 120%) and placed in the centrifuge container. It was incrementally consolidated one-dimensionally to a maximum vertical stress of 500 kPa, and later decreased to 250 kPa. Measurements made during consolidation indicated a coefficient of consolidation of $0.2\,mm^2/s$. The day before testing, pore pressure transducers were pushed into the kaolin around the tunnel cavity. The sand layer was made by compacting Oakamoor sand, mixed at a water content of 8%, in a rectangular mould. Targets were pushed into the frontal face of the sample and the mould closed. It was then

placed in a freezer. This sand freezing method allowed reasonably consistent sand layers to be produced without disturbing the lower clay layer. For tests involving a model wall, a spacer was placed in the mould and sand compacted around. The spacer was removed and replaced by a wall during the model making process.

On the day of testing, the strongbox was taken from the press, its front side removed, the tunnel cavity cut and lined with the rubber bag, targets pressed into the front face of the kaolin and the perspex window placed, which closed the container and allowed viewing of the model during test. The window was always greased by silicone fluid to minimize the frictional contact with the soil. Finally, the frozen sand sample, model wall and LVDTs were placed on the kaolin surface. During each stage of the model preparation all surfaces of the kaolin sample were covered by a really thin layer of silicone fluid to avoid water evaporation, with the exception of the upper surface where the frozen sand was placed. In fact, it was important to minimize the time required for this procedure, also to avoid the effect due to de-freezing and losing material. Once the container was on the swinging platform, the centrifuge test began. The inertial acceleration was increased from 0 g to the maximum value required of 160 g while the air pressure applied inside the tunnel cavity was increased to match the increase of in situ stress at tunnel axis level. All drainage connections were open to allow water from the standpipe to reach the base drainage layer. The hydraulic conditions were maintained constant during the centrifuge tests, with the water level set at about 25 mm above the sand/clay interface. The new equilibrium of pore pressure in the kaolin was achieved quite rapidly due to the presence of the base drainage layer and upper sand layer. The excavation process was simulated by reducing tunnel air pressure at a rate of about 85 kPa/min, while data from transducers and digital images were recorded every second.

3 LITERATURE BACKGROUND

This section will present previous works on tunnelling excavation, for greenfield condition, mainly focusing on the field of ground displacements for uniform ground: just few references are available on the field of ground strains and on the assessment of structure damage for the case of a completely buried wall for both uniform and layered soils, indeed.

3.1 *Surface ground settlements*

Around a tunnel, vertical displacements are given by a Gaussian distribution (O'Reilly & New 1982):

$$S_v = S_{v\,max}\, exp\left(-\frac{x^2}{2i_0^2}\right) \tag{1}$$

where S_v = vertical displacement; $S_{v\,max}$ = maximum settlement at the tunnel centreline; x = horizontal distance from tunnel centreline; and i = distance from tunnel centreline to the inflexion point of the settlement trough.

The volume loss, V_L, is defined as percentage of the nominal volume of the tunnel cavity. V_S, is the volume of the settlement trough from Equation 1. For settlements in the (undrained, zero volumetric strain) clay layer it is similarly expressed as a percentage of the nominal tunnel volume. Under these conditions, $V_L = V_S$.

A number of relationships are suggested to determine the parameter of settlement trough, i. A linear relationship where i is independent of the tunnel diameter (e.g. Eq. 2) or other formula (i.e. Eq. 3):

$$i_0 = kz_0 \tag{2}$$

$$i_0 = 0.5D^{0.2} z_0^{0.8} \tag{3}$$

where z_0 = depth of tunnel axis from ground surface; k is a parameter that depends on the soil – about 0.4 for strong clay and sand below water level, 0.7 for soft clay, and 0.2–0.3 for sand above water level –; and D = tunnel diameter.

Surface settlements in sandy ground may be given by other expressions, e.g. Jacobsz (2002):

$$S_v = S_{v\,max}\, exp\left(-\frac{1}{3}\left(\frac{|x|}{i}\right)^{1.5}\right) \tag{4}$$

which gives a steeper curve and smaller values of S_v.

On the contrary, for layered ground problems, only the following relationship is available, with no clear evidence of the real trough width from in situ measurements especially for a drained stratum overlaying an undrained, fine-grained layer:

$$i_0 = \sum k_i z_i \tag{5}$$

where k_i = parameter connected to the specific soil as defined above; and z_i = thickness of the soil.

3.2 *Subsurface ground settlements*

Guidelines for subsurface settlements are usually an extension of those discussed for surface settlements: new relationships are suggested in order to define different values of parameters at every depth. From Equation 2, a linear trend has been suggested as:

$$i_z = k(z_0 - z) \tag{6}$$

where all terms have already been introduced. Thus, it is important to assess the k factor. Few approaches are suggested in the literature: O'Reilly & New (1982)

use a constant value for k whereas Mair et al. (1993) give a non-linear trend:

$$k_z = \frac{0.175 + 0.325(1 - z/z_0)}{1 - z/z_0} \quad (7)$$

for a uniform undrained ground, this equation also give a linear trend of i_z.

Otherwise, a non linear trend of i_z (Moh et al. 1996) could be taken into consideration:

$$i_z = bD\left(\frac{z_0 - z}{D}\right)^m \quad (8)$$

where i_z = distance of point inflexion from tunnel centreline; z_0 = depth of tunnel axis from ground surface; z = depth of the specific horizon from ground surface; D = tunnel diameter; m = parameter that depends on the soils, 0.4 for drained soil, 0.8 for undrained, fine grained soil; and b = parameter that also depends on the soils.

It is interesting to note that the easiest relationship (Eq. 6) always underestimates the width of the settlement trough and overestimates the maximum vertical displacement above the tunnel axis.

3.3 *Horizontal displacements*

In order to assess damages induced to pre-existing structures, it is important to define horizontal displacements as well. At each horizon, they can easily define by the following equation:

$$S_h = \frac{x}{H} S_v \quad (9)$$

where S_h = horizontal displacement; S_v = settlement at the same depth; x = horizontal distance from tunnel centreline; and H = focus of displacement vectors – i.e. the point on the tunnel centreline to which displacement vectors from a horizon are directed.

For undrained conditions, Equation 1 and 2 imply that displacement vectors will be directed at the tunnel axis. On the contrary, assuming the linear trend of i_z from Equation 7 and undrained, zero volumetric strain conditions, with the exception of few horizons either very close to the ground surface or near the tunnel crown, the focus is always to the same point below the tunnel axis – i.e. the intersection between the tunnel centreline and the tangent to the i_z trend. No references are available for drained soils.

4 RESULTS

4.1 *Displacements and strains of ground*

In this section results from the most significant tests undertaken will be presented: the reference test of the greenfield condition and two tests on the interaction problem, the one using the weakest wall and that using the strongest wall. Data from each test, at every horizon, have been analyzed at some fixed reference values of volume loss (V_L = 5.0%–10.0%–15.0%–20.0%) assessed in the kaolin stratum, where the soil is under undrained conditions with no volumetric strains. In fact, it is quite evident that horizons from kaolin layers should give the same volume loss at the same instant, while the sand layer, which is under drained conditions, shows smaller values of volume loss due to dilation.

At first, settlements were plotted for all different horizons, in order to check if a Gaussian distribution could really fit the experimental data, for the range of volume loss discussed above. They are values of V_L bigger than the usually ones generated in practice gy shield tunnelling machines, but the precision of image processing was not accurate enough to use smaller values of volume loss. The distance i_z for the settlement troughs was evaluated at every horizon, both in sand and in clay, and was found to remain constant at each horizon during the process of simulated tunnel excavation. Thus the patterns of movement should be independent of magnitude of volume loss so allowing movements at what are relatively high values of volume loss to be used in analysis. Horizontal displacements were analyzed as well and fitted by using Equation 9, once the focus of displacement vectors, H, had been assessed at every horizon. H changes with the depth and a different value can be assigned for every horizon in the model. In the sand, H is constant for a particular horizon and is independent of the horizontal distance from the tunnel centreline, x. However, for a particular horizon in the clay, H is constant just for the range $-i \le x \le i$ and linearly decreases with x. Figure 2 shows that the Gaussian distribution and

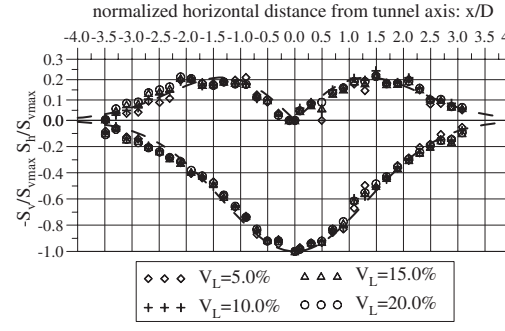

Figure 2. Typical experimental data from centrifuge testing and their interpolation by cross-hatched lines: normalized distance from tunnel axis (x/D) against normalized horizontal displacement ($S_h/S_{v\,max}$) and vertical displacement ($-S_v/S_{v\,max}$).

the relationship suggested by Equation 9, fit well all experimental data.

All values of i_z and H can be plotted against depth, in order to assess trends for the greenfield test and ground-structure interaction tests.

From Figure 3 it is evident that theoretical trends suggested from the literature always underestimate the values assessed from experimental data, both on the ground surface and subsurface. In contrast to the greenfield data, the wall placed within the upper sand layer evidently makes the settlement troughs wider in sand because it has a connection with widespread parts of the ground. The maximum settlement above the tunnel axis is therefore smaller for the case of the ground-structure interaction configuration, because all parameters have been evaluated at constant values of volume loss as previously explained. All data can well be fitted by using Equation 8, resulting in values of m typical of drained soils. It is interesting to note that there are no evident differences between the behaviour of the weak wall and the strong wall. Figure 4 presents the focus H of displacement vectors: it increases with the depth in the sand layer, but decreases for the clay stratum and it could be fitted by exponential functions for all tests. This inversion is very clear and emphasizes the significant effect of the sand/clay interface. At the interface the H focus tends to a horizontal asymptote as denoted by the thick line: Figure 5 shows that at this depth displacement vectors are almost vertical. In this instance, the strong wall makes the vector focal point for the sand deeper in comparison to the ones from greenfield and weak wall tests.

Various ground strains, including vertical, horizontal, shear, principal and their directions, volumetric and maximum shear strains have been evaluated.

Figure 6 presents contours of volumetric strains from the greenfield test. The thick black line marks the zero strain contours, the dashed horizontal line represents the sand/clay interface, while the white hatch shows ground compression, and the dark hatch denotes dilation. The soil above the tunnel crown experiences a decrease in volume, whereas soil in other locations within the clay layer shows negative volumetric strains. It is possible to distinguish the widespread compressive behaviour within the sand layer, apart from the two lateral zones of negative volumetric strains at the ground surface, far from the

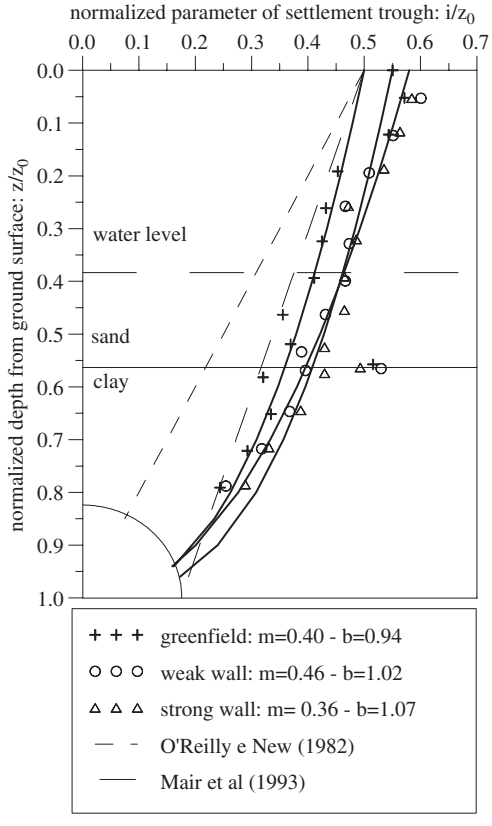

Figure 3. Normalized parameter of settlement trough (i/z_0) against normalized depth from ground surface (z/z_0).

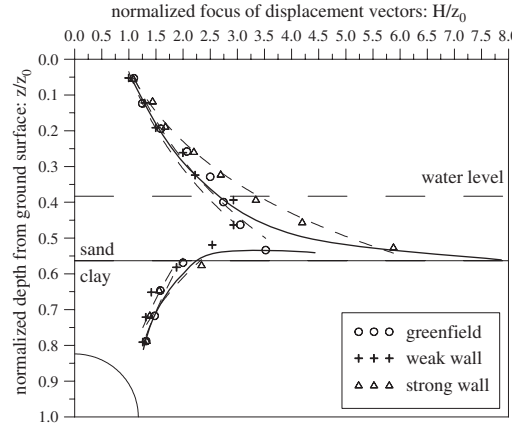

Figure 4. Normalized focus of displacement vectors (H/z_0) against normalized depth from ground surface (z/z_0).

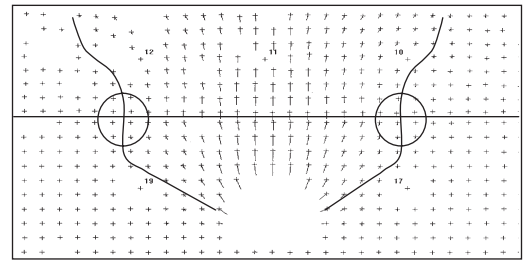

Figure 5. Ground displacement vectors around the tunnel.

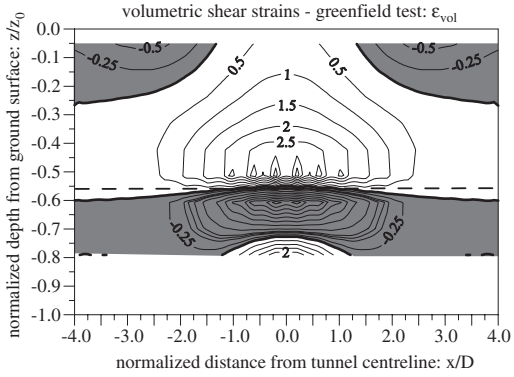

Figure 6. Greenfield test: contours of volumetric strain, compression is positive ($V_L = 20.0\%$).

tunnel centreline. It is worth to notice that a dilative behaviour can be assessed at the bottom of the sand layer, which is confirmed by values of volume loss smaller than the reference ones in clay. Also, the maximum settlements at the tunnel centreline from the ground surface to the sand/clay interface first increase and later decrease just close to the interface. A similar shape of contours is evident in Figure 7 for the weak wall test: negative strains in clay are localised close to the tunnel centreline only. Whereas the strong wall performed a quite different behaviour. Strains of similar magnitude were observed in the different tests: at a volume loss of 20.0%, greenfield, $-4.7\% \leq e_{vol} \leq 3.8\%$; weak wall test, $-2.8\% \leq e_{vol} \leq 4.1\%$; strong wall test, $-0.4\% \leq e_{vol} \leq 1.0\%$. As a consequence of the connection with the wall, volumetric strains decrease from the greenfield to the strong wall condition.

Finally, Figure 8 shows contours of maximum shear strains for the greenfield condition. It is evident that the biggest values of shear strains are close to the tunnel cavity where the major unloading occurs. Moreover contours seem to narrow at the sand/clay interface and widen in the sand layer from the bottom to the top. Two vertical bands tend to connect zones of intense shear straining near the tunnel crown to zones of significant shear strains within the sand layer. Maximum shear strains in the wall-ground interaction tests are similar both in shape and in magnitude: greenfield test, $\gamma_{max} < 12.3\%$; weak wall, $\gamma_{max} < 7.2\%$; and strong wall, $\gamma_{max} < 8.5\%$.

4.2 *Effect on pre-existing structure*

Only few LVDTs were used to measure the settlements of the model-wall just in a restricted number of points and there are no data available of horizontal displacements and field of strains.

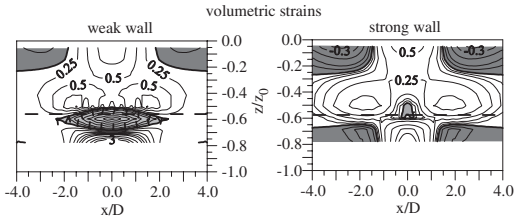

Figure 7. Wall-ground interaction tests: contours of volumetric strains ($V_L = 20.0\%$).

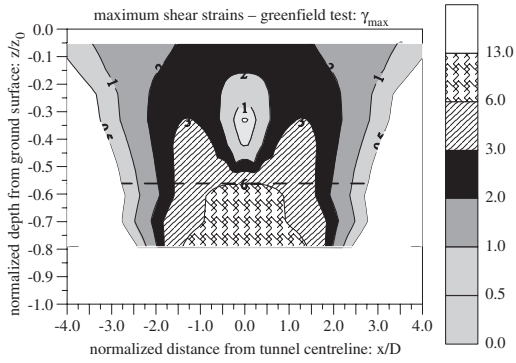

Figure 8. Greenfield test: contours of maximum shear strain ($V_L = 20.0\%$).

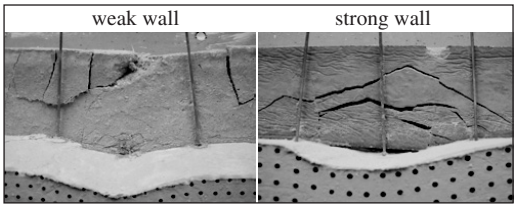

Figure 9. Failure mechanism of model-walls tested.

The model-wall was completely buried within the sand layer and it was not possible to assess its damage in terms of magnitude of strains. But, LVDTs gave information about the stage when the wall likely to have cracked and it is especially significant to show pictures taken after centrifuge tests, once the sand was removed and the failure mechanism clearly appeared. Figure 9 presents these pictures for both the weak and strong wall: in the left side of the figure the effect of bending deformation causing cracking due to direct tensile strain is seen. In contrast, the strong wall is characterized by a shear deformation with cracking due to diagonal tensile strains. Literature references suggest these deformations as the two extremes for modelling the structure as a simple beam under a deflected shape. Finally, during centrifuge testing the weak model-wall

was always in contact with the upper surface of kaolin, which did not occur in the strong wall test.

5 CONCLUSIONS

Few guidelines are available from the literature on tunnelling in layered ground, especially for subsurface behaviour of drained (sand) soil. The centrifuge results demonstrate the significant effect of the presence of a drained soil overlying an undrained stratum both in terms of trend with depth of the horizontal distance to the point of inflexion, i, and the H focal point. The ground displacement data can be fitted by a Gaussian distribution and important information results from the assessment of its strains.

Important evidence has been produced about changes due to the ground-structure interaction when the wall was modelled, even if no detailed information was obtained about the general pattern of displacements and strains. The failure mechanism of the structures could be observed, which indicated two different failure modes: by bending deformation and by shear deformation.

REFERENCES

Grant, R.J. 1998. *Movements Around a Tunnel in Two-Layer Ground.* PhD Thesis, City University, London, UK.

Jacobsz, S.W. 2002. *The effects of tunnelling on piled foundations.* PhD Thesis, University of Cambridge, UK.

Mair, R.J., Taylor, R.N. & Bracegirdle, A. 1993. Subsurface settlement profiles above tunnels in clays. *Géotechnique* 43, No 2: 315–320.

Moh, Z.-C., Hwang, R.N. & Ju, D.H. 1996. Ground movements around tunnels in soft ground. *Proc. Int. Symposium on Geotechnical Aspects of Underground Construction in Soft Ground, London.* Mair & Taylor (eds): 725–730.

O'Reilly, M.P. and New, B.M. (1982). Settlements above tunnels in the United Kingdom – their magnitude and prediction. *Tunnelling '82*. London, IMM, pp. 173–181.

Taylor, R.N. 1995. *Geotechnical Centrifuge Technology.* Blackie Academic & Professional.